AN EXPERIMENTAL INVESTIGATION INTO CARBON AS A SPACE WEATHERING PRODUCT ON MERCURY AND CARBONACEOUS ASTEROIDS.

A. Shackelford[1], K. L. Donaldson Hanna[1], J. Gillis-Davis[2], Z. Rahman[3], B. A. Cymes[3], R. Christoffersen[3], L. P. Keller[4]. [1]University of Central Florida, 4111 Libra Drive, Orlando, FL 32816, [2]Washington University, One Brookings Drive, St. Louis, MO 63130, [3]Amentum, NASA Johnson Space Center, Houston TX, 77058, [4]NASA Johnson Space Center, Houston TX, 70058. (autumn.shackelford@ucf.edu).

Introduction: Carbon is hypothesized to be present as a darkening agent on the surface of Mercury and on carbonaceous asteroids [e.g., 1, 2]. On Mercury, this carbon may exist as exogenic material introduced by impactors [3] or as endogenic material excavated from a theorized graphite floatation crust [1]. Within Mercury's low-reflectance material (LRM), carbon may be present in concentrations as high as 5 wt. % [4]. Carbonaceous chondrite meteorites ascribe a wide range of carbon contents for C-type asteroid parent bodies, from 0.1 to 5 wt. % [5]. Could the presence of carbon on these bodies, coupled with a harsh space weathering environment, cause the formation of nano- or microphase carbon within silicate regolith particle rims?

Space weathering is most well understood in the lunar and S-type asteroid perspective, where nanophase iron (npFe) is known to be the cause of increasing optical maturity (spectral reddening, an overall darkening, and decreasing prominence of spectral features) [e.g., 6, 7], but not every planetary surface is dominated by iron-bearing minerals. Mercury's low-Fe surface is of particular interest in this work. Absorption features due to Fe^{2+} in visible-to-near-infrared (VNIR) spectra of the Mercurian surface have yet to be observed [e.g., 8]. Gamma-ray and X-ray data also confirm that Mercury's surface is low in surficial iron [e.g., 9, 10]. While npFe is an unlikely (but not impossible [e.g., 11]) contributor to surface darkening, recent experiments show that graphite may be a possible component in Mercurian space weathering products [12].

To better understand the role carbon may play in space weathering on Mercury and C-type asteroids, we have used pulsed laser irradiation to simulate aspects of micrometeorite bombardment on powders of low- to no-iron silicates mixed with various C-bearing opaques. We present VNIR reflectance spectra from 0.3-2.5 µm of each mixture before and after irradiation, as well as preliminary transmission electron microscopy (TEM) and energy dispersive X-ray spectroscopy (EDS) analyses of select samples.

Samples and Methods: *Sample Suite.* Each powdered mixture consists of 95 wt. % of one base silicate and 5 wt. % of one opaque, added in accordance with the carbon abundances in Mercury's LRM outlined in Klima et al. [4]. We chose three silicate analogs for this work: (1) San Carlos olivine (SCO), for its frequent use in space weathering experiments [e.g., 13, 14], (2) synthetic forsterite, and (3) synthetic enstatite. Both synthetics were produced by Matexcel (a materials science company) and are iron-free. We also chose three opaques to mix with each silicate, as each C-opaque has different spectral signatures: (1) Carbon black, a common choice for simulated carbonaceous asteroid weathering [e.g., 15], (2) anthracitic coal, for its low volatile content compared to other coals, and (3) graphite, for Mercury's possible graphite crust [1].

Simulated Space Weathering. We simulated aspects of micrometeorite bombardment on our samples using the Washington University Laser Space Weathering Laboratory, which uses two lasers of differing pulse lengths to recreate the full thermal event of a micrometeorite impact in the inner Solar System [16]. Each sample was weathered at ~10^{-7} torr for the amount of time (or equivalent irradiation) it takes for San Carlos olivine to reach VNIR optical maturity [7] with this experimental setup. We irradiated the three base silicates and the nine silicate and carbon mixtures to generate a total of 12 weathered samples.

Results: *VNIR Results.* VNIR endmember spectra for the silicates and opaques are presented in **Figure 1** to highlight the starting reflectance values and differences in spectral slope and absorption features.

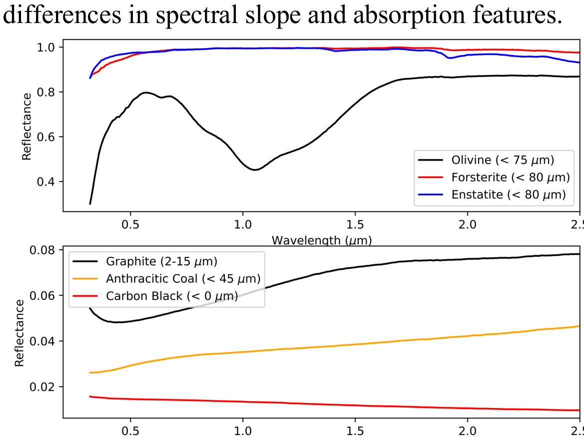

Figure 1. Endmember spectra of silicates (top) and opaques (bottom). Note the lack of 1-µm feature for the synthetics and spectral slope and albedo of the opaques.

VNIR spectra of all mixtures before and after irradiation are presented in **Figure 2**. The base silicate spectra are omitted for clarity so that the changes in spectral features, slope, and reflectance can be seen more readily. For the irradiated SCO mixtures, we see a decrease in prominence/near-complete removal of the 1-µm feature. For all irradiated mixtures, we see spectral darkening and reddening. The visible slope (0.4-0.55 µm) and near-infrared slope (1.7-2.5 µm) appear to be independent instead of sharing a consistent "blue" or "red" slope across the VNIR range. Despite the independence between the visible and NIR regions, "bluer" starting slopes almost always shift to become "redder" after irradiation in both the visible and the NIR.

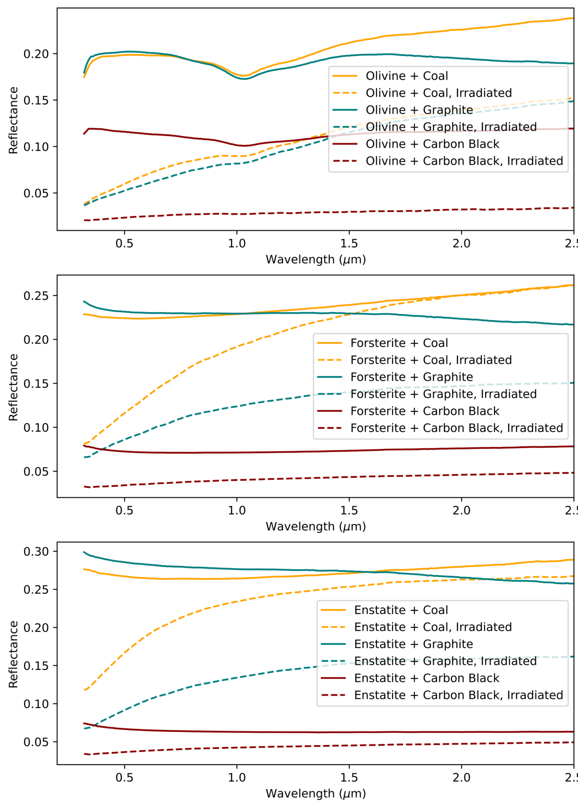

Figure 2. VNIR spectra of San Carlos olivine (top), forsterite (middle), and enstatite (bottom) mixtures before and after irradiation. Note the different scales for reflectance on the y-axis for each plot.

Preliminary TEM results. Samples were prepared using a Quanta 3D-FEG focused ion beam (FIB) system and analyzed using a JEOL 2500SE TEM. To compare this experimental setup against existing experiments, we chose to study our weathered base SCO sample first. TEM and EDS data show a variety of features within the melt generated by the lasers, including 10-100 nm metallic npFe of varying sizes and concentrations, vesicles, and regions of olivine recrystallization (**Figure 3**). We also performed TEM and EDS on our weathered enstatite and carbon black mixture. Analyses revealed melt with a higher Mg content than the bulk, vesicles, and 8-10 nm nanophase inclusions. The inclusions may be carbonaceous opaques or potentially vesicles; the EDS data were inconclusive (**Figure 4**).

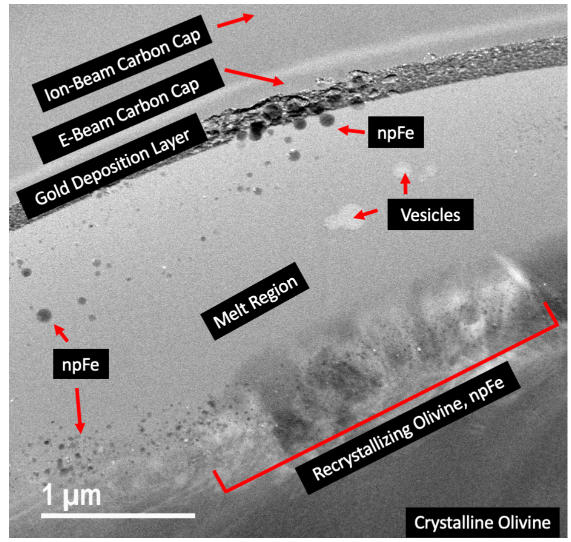

Figure 3. High-angle annular dark-field (HAADF) scanning TEM image of a FIB cross-section taken from a singular weathered SCO particle.

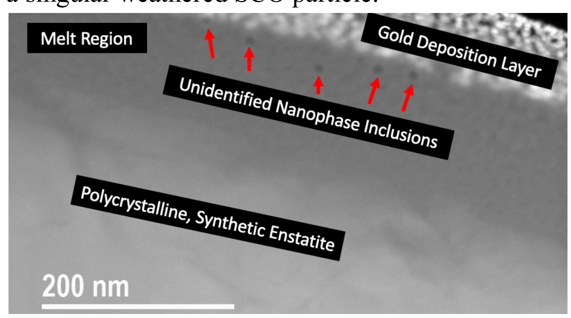

Figure 4. Scanning TEM image of a FIB cross-section taken from a polycrystalline enstatite particle in the weathered enstatite and carbon black mixture.

Acknowledgments: Spectra were obtained by Dr. Takahiro Hiroi at the RELAB facility at Brown University. FIB preparation and TEM/EDS analysis were performed with and supported by the NASA Facility for Astromaterials Research at Johnson Space Center under NFAR_2024_0028. This work was also directly supported by NASA's Solar System Exploration Research Virtual Institute cooperative agreement notice 80NSSC19M0214 for the Center for Lunar and Asteroid Surface Science (CLASS).

References: [1] Vander Kaaden & McCubbin (2015) *JGRP, 120,* 195-209. [2] Vilas and Hendrix (2020) *AGU 2020*. [3] Bruck Syal et al. (2015) *Nat. Geo., 8,* 352-356. [4] Klima et al. (2018), *GRL, 45,* 2945-2953. [5] Glavin et al. (2018), *Prim. Met. and Ast.,* 205-271. [6] Pieters & Noble (2016) *JGRP, 121,* 1865-1884. [7] Cudnik (2023) *Springer,* 943-949. [8] Warell et al. (2006) *Icarus, 180,* 281-291. [9] Evans et al. (2012), *JGRP,* 117(E12). [10] Weider et al. (2014), *Icarus,* 235, 170-186. [11] Nobel & Pieters (2001). [12] Bott et al. (2024), *PSJ, 5,* 248. [13] Weber et al. (2020) *EPS Let., 530.* [14] Jaramillo-Correa et al. (2024) *PSJ, 5:229.* [15] Kanuchova et al. (2012) *Icarus, 221,* 12-19. [16] Gillis-Davis (2022) *EPSC 2022, #1193.*